

B. Noise Figure

The flick noise and thermal noise current generated by a MOSFET are as equation (1) and (2) respectively [2]. They are both functions of g_m . When the MOSFET is cut off, the noise can be negligible. Since the LO switches the transconductance stages periodically, only half of the transconductor MOSFETs are switched on at one time. Though the number of the transconductor MOSFETs doubles in the switched transconductor topology, the noise introduced is just the same as the conventional topology.

$$\overline{i_{n,1/f}^2} = \frac{K}{C_{ox}WL} \frac{1}{f} g_m^2 \quad (1)$$

$$\overline{i_{n,thm}^2} = 4kT\gamma g_m \quad (2)$$

In the switched transconductor topology, the noise current generated by the switches is in common mode, because the two MOS transistors from one transconductant pair are working at the same state. Then the noise will be cancelled in the differential outputs. But in the conventional topology, the situation is totally different. Each switch transistor will contribute notable output noise [3]. That's why the switched transconductor topology has lower NF.

The approximate SSB NF of Gilbert mixers in Figure.1 (a) has been derived as equation (3) [4], where the α and c are LO related parameters, and γ , r_g and g_m denote the noise factor, gate resistance and transconductance respectively.

$$NF_{SSB} = \frac{\alpha}{c^2} + \frac{2(\gamma_5 + r_{g5}g_{m5})g_{m5}\alpha + 4\gamma_1\overline{G_1} + 4r_{g1}\overline{G_1} + 1/Z_L}{c^2 g_m^2 R_s} \quad (3)$$

Since the noise generated by the switch is cancelled, the SSB NF of the switched transconductor topology can be derived as equation (4) [1].

$$NF_{SSB} = \frac{\alpha}{c^2} + \frac{2(\gamma_1 + r_{g1}g_{m1})g_{m1}\alpha + 1/Z_L}{c^2 g_m^2 R_s} \quad (4)$$

C. Linearity

When the transconductance stage is switched on, the common-source node of it is at low voltage. So, the

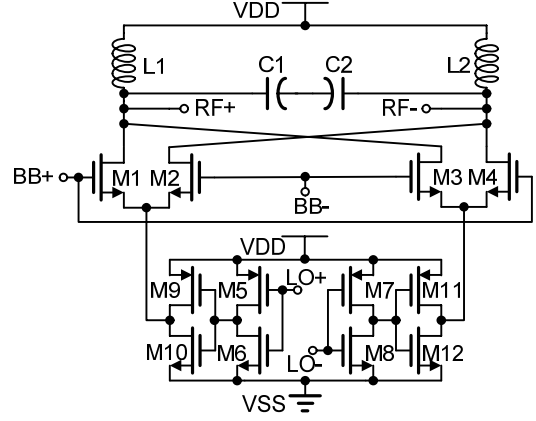


Figure.2. Schematic of the upconversion mixer

NMOS of corresponding inverter is at linear region, acting as a resistor R_o . The output differential current can be derived as equation (5) [1], where the g_1, g_2 and g_3 denote the Taylor coefficients derived from the I-V of the MOSFET.

$$i_o = g_1 v_{RF} + \left(\frac{g_3}{4} - \frac{g_2^2 R_o}{1 + 2g_1 R_o} \right) v_{RF}^3 \quad (5)$$

Though g_3 is negative when the MOSFET is in strong inversion, the deterioration of the linearity resulted from R_o can be negligible if R_o is small enough.

III. UPCONVERSION MIXER DESIGN

Figure.2 shows the schematic of the low noise high linearity upconversion mixer. To achieve better switching, the size of the inverter should be increased. Out of question, that will lead to larger power dissipation. To solve this problem, two inverters with small size are cascaded to replace the single inverter switches. And the inverters with small size make the VCO design easier, reducing the driving capability requirement.

LC tank is employed as output loads, as the output signal is narrow RF band. There's no expense of any DC voltage headroom, So that the mixer can work in the low voltage power supply. In this design, a center-tapped differential inductor [5] is implemented, instead of two independent inductors to saves the chip area. The differential equivalent parallel resistance of the LC tank can be as high as 1k ohms, which reduce the requirement of g_m to achieve given conversion gain (CG). According to equation (6), the over drive voltage of the transconductance NMOS can be large, leading to good

linearity.

$$V_{GS} - V_T = \frac{2I_{DS}}{g_m} \quad (6)$$

IV. SIMULATION AND MEASUREMENT RESULT

The chip is implemented in SMIC 0.18- μm RF CMOS process. Figure.3 is the photograph of the chip after bonding and the test PCB board. The chip size including IO pads is 0.63mm \times 0.78mm. And it consumes 10mA current at 1.8V power supply on average. The chip is COB packaged to reduce the affect of parasitics. The power supply VDD is connected to the corresponding pad on the PCB via three bonding wires to reduce the parasitic inductance, which will deteriorate the RF performance of the circuit.

The 900MHz LO is given to measure the performance of the mixer chip. Figure.4 shows the simulated and measured conversion gain. The resonant frequency of the LC tank is about 50MHz away from simulation, and the Q factor is a little smaller so that the curve is more flatten.

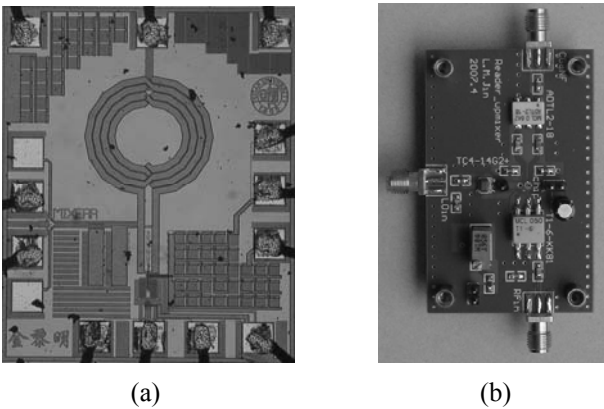


Figure.3. Photograph of (a) the chip (b) the PCB

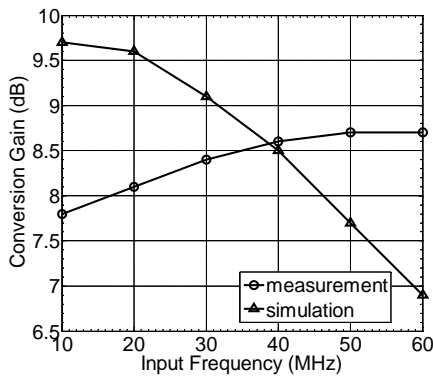


Figure.4. Simulated and measured CG

The input referred third-order intercept point (IIP3) is measured with the two-tone test at 9.5MHz and 10.5MHz. Figure.5 shows the output spectrum when the power level of every input tone is -11dBm. The central two peaks are the two-tone signals, while the side two peaks are the third order intermodulation products. Figure.6 shows measured IIP3 with input level sweeping. Though the output is attenuated due to impedance mismatch, the IIP3 is not impacted absolutely, since it lies on the difference between the 1st and 3rd order. The measure IIP3 is 10.5dBm, while the simulated IIP3 is 12dBm.

Figure.7 shows the simulated and measured NF with output buffer, which will heighten NF by about 0.5dB. The measured SSB NF is about 11dB.

Table I gives the measurement results of the designed mixer compared with several published works. It can be seen that the NF and IIP3 performance of this work are more competitive. It should be noticed that SSB NF is 3dB larger than DSB NF commonly.

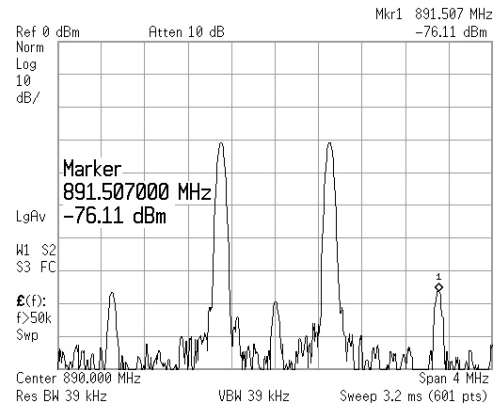


Figure.5. Spectrum of two-tone measurement

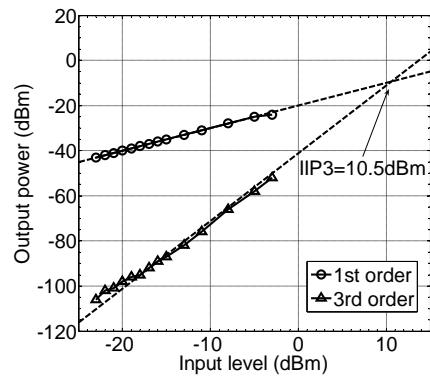


Figure.6. Measured IIP3

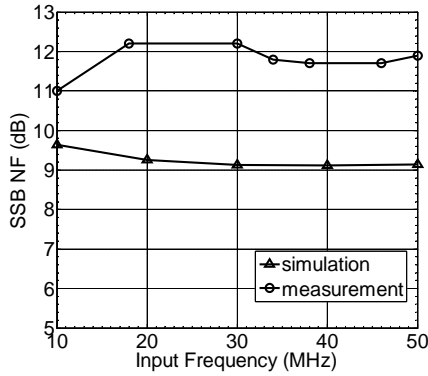


Figure.7. Simulated and measured NF

V. CONCLUSION

In this paper, an upconversion mixer exploiting a switched transconductor topology is designed and measured. The advantage of the topology in NF and IIP3 is analyzed compared with the conventional one. The measurement result shows that the designed mixer achieved high gain, low NF and high IIP3.

ACKNOWLEDGMENT

The authors would like to thank Dr. Haiyang Hu at Agilent Technologies providing necessary instruments for measurements, and thank Lu Yuan, Ronghua Ni, Lei Lu, Zhenyu Yang, Youchun Liao and Xi Tan for many

helpful discussions.

REFERENCES

- [1] E.A.M. Klumperink and S.M. Louwsma, "A CMOS switched transconductor mixer," *IEEE J. Solid-State Circuits*, vol. 39, pp. 1231-1240, Aug. 2004.
- [2] B. Razavi, *Design of analog CMOS integrated circuits*, McGraw-Hill, 2001.
- [3] H. Darabi and A.A. Abidi, "Noise in RF-CMOS mixer: A simple physical model," *IEEE J. Solid-State Circuits*, vol. 35, pp. 15-25, Jan. 2000.
- [4] M.T. Terrovitis and R.G. Meyer, "Noise in current-commutating CMOS mixers", *IEEE J. Solid-State Circuits*, vol. 34, pp. 772-783, Jun. 1999.
- [5] Lei Lu and Zhangwen Tang, "Equivalent model and parameter extraction of center-tapped differential inductors," *Chinese journal of semiconductors*, vol. 27, pp. 2150-2154, Dec. 2006.
- [6] Lu Liu and Zhihua Wang, "Analysis and design of a low-voltage RF CMOS mixer," *IEEE Trans. CAS II*, vol. 3, pp.212-216, Mar. 2006.
- [7] H. Darabi and J. Chiu, "A noise cancellation technique in active RF-CMOS mixers," *IEEE J. Solid-State Circuits*, vol. 40, pp. 2628-2632, Dec. 2005.

Table I

Summary of measurement results and performance comparison

	[1]	[6]	[7]	This work
Process	0.18- μ m CMOS	0.18- μ m CMOS	0.13- μ m CMOS	0.18- μ m CMOS
Gain (dB)	10	6.6	1	8
NF (dB)	24 (DSB)	21 (SSB)	11.8 (DSB)	11 (SSB)
IIP3 (dBm)	6	1.5	11	10.5
Power	0.6mW	N/A	2mA \times 1.2V	10mA \times 1.8V
Die area (mm ²)	0.075 \times 0.065 (core)	N/A	0.08 \times 0.15	0.63 \times 0.78